European Journal of Medicinal Chemistry 70 (2013) 887–900

Contents lists available at ScienceDirect

European Journal of Medicinal Chemistry

journal homepage: http://www.elsevier.com/locate/ejmech

Original article

Designing and synthesis of novel antimicrobial heterocyclic analogs of fatty acids

Aiman Ahmad [a], Anis Ahmad [b], Himani Varshney [a], Abdul Rauf [a,*], Mohd Rehan [c,1], Naidu Subbarao [c], Asad U. Khan [b,**]

[a] Department of Chemistry, Aligarh Muslim University, Aligarh 202002, India
[b] Interdisciplinary Biotechnology Unit, Aligarh Muslim University, Aligarh 202002, India
[c] School of Computational and Integrative Sciences, Jawaharlal Nehru University, New Delhi, India

ARTICLE INFO

Article history:
Received 28 June 2013
Received in revised form
14 October 2013
Accepted 21 October 2013
Available online 27 October 2013

Keywords:
1,3-Dipolar-cycloaddition
Fatty acid
Mode of action

ABSTRACT

Novel series of long chain isoxazole derivatives were designed as inhibitors of Cytochrome P450-14DM14a-demethylase from *Candida albicans* and ribosomal subunit of S12 protein from *Escherichia coli*. The novel compounds (**6**–**10**) were synthesized through 1,3-dipolar cycloaddition of nitrile oxide to long chain alkynoic acid and alkenyl/hydroxyalkenyl esters and tested for their antimicrobial activity by disk diffusion assay and MIC by broth micro dilution method. After predicting the hidden potential and drug-likeness of compounds, ADMET-related descriptors were also calculated to predict pharmacokinetic properties. Molecular docking studies have been performed to evaluate possible mode of action of molecules in active site of receptor. Compounds (**9** and **10**) showed excellent antimicrobial activity nearly equivalent to the control compounds.

1. Introduction

The enteric bacterial infections are one of the major factors of morbidity in developing countries including Indian sub-continent, part of South America and tropical part of Africa [1]. The common gram-positive pathogens of nosocomial infections are *Staphylococcus aureus* which may also account for outbreaks [2,3]. The world's most common and serious infectious diseases like invasive dysentery and diarrhea are caused by *Escherichia coli* [4,5]. Amoxicillin, norfloxacin and ciprofloxacin are generally used to treat the infections caused by the *E. coli* but they have some side effects [6]. The important role in the treatment failure is played by toxicity and resistance to the drugs also [7]. Several severe diseases may be caused by gram negative and positive bacteria which may lead to huge damage of host tissues [8]. More than 90% of the cases of vaginitis are of candidiasis, trichomoniasis and bacterial vaginosis [9].

Lipophilicity is the key physicochemical parameter linking membrane permeability and hence drug absorption and distribution with the route of clearance (metabolic or renal) [10,11]. The biological activity spectra of these compounds obtained by PASS online (http://www.pharmaexpert.ru/PASSOnline/index.php) estimates the predicted activity spectrum of a compound as probable activity (Pa) and probable inactivity (Pi) [12,13].

Nitrogen and oxygen containing heterocyclic compounds have received considerable attention due to their wide range of biological and pharmacological activities. Among the family of heterocyclic compounds the five membered isoxazoles and isoxazolines/dihydroisoxazoles provide a valuable scaffold in medicinal chemistry as well as a useful synthon in organic synthesis. Isoxazoles and isoxazolines have been reported to possess antitubulin as well as anti-inflammatory activity [14,15]. Dihydroisoxazole derivatives are reported as antinociceptive compounds [16]. In addition, isoxazoline derivatives have played a crucial role in the theoretical development of heterocyclic chemistry and are also used extensively in organic synthesis [17]. Also, medicinal activity like anxiolytic activity has been reported for isoxazole derivatives [18]. So many methodologies exist towards the synthesis of isoxazoles [19,20] and dihydroisoxazoles [21] and most of them endeavor nitrile oxide cycloaddition as a keystep [22]. The addition of a 1,3-dipole to an alkene/alkyne for the synthesis of 5-membered ring is a classic reaction in organic chemistry. The general application of 1,3-dipoles in organic chemistry was first established by Huisgen in

Abbreviations: MR, molar refractivity; MW, molecular weight; MV, molecular volume; PASS, predicted activity spectrum of substances; PSA, polar surface area; SAR, structure–activity relationship; MIC, minimal inhibitory concentration; MRSA, methicillin resistant *Staphylococcus aureus*; Sa, *Staphylococcus aureus*.

* Corresponding author. Tel.: +91 9412545345.
** Corresponding author.
E-mail address: abduloafchem@gmail.com (A. Rauf).
[1] Present address: King Fahd Medical Research Centre, King Abdulaziz University, Jeddah 21589, Saudi Arabia.

0223-5234/$ – see front matter © 2013 Elsevier Masson SAS. All rights reserved.
http://dx.doi.org/10.1016/j.ejmech.2013.10.051

1960s [23]. Isoxazole and isoxazoline heterocycles are derived from the [3 + 2] cycloaddition of a nitrile oxide to an alkene and alkyne, respectively [24]. The nitrile oxide 1,3-dipole is generated in situ in Mukaiyama reaction from the corresponding primary nitroalkane and phenyl isocyanate [25]. Here, nitrile oxide is generated by dehydration of primary nitroalkanes. This method is however the most useful due to its easy set up as described by Mukaiyama in 1960 [25], 1,4-phenylene diisocyanate was used as dehydrating agent [26]. By using 1,4-phenylene diisocyanate, polyurea byproduct was obtained which may be removed from product by simple filtration because this polyurea byproduct was insoluble in the reaction solvent (benzene and tetrahydrofuran). Various biological applications such as antimicrobial [27], pesticidal [28], anticancer [29] and antifungal activities [30] have been reported for seed oils, long chain alkenoic acids and their derivatives. These observations and our interest in the chemistry of heterofatty acids prompted us to synthesize isoxazole derivatives of fatty acids with different substituent at 4- and 5- positions. For this reason, the present strategy for the synthesis of new compounds is aimed in the direction of developing new isoxazole derivatives to inhibit the growth of gram-positive, gram-negative bacteria and most pathogenic fungi. After synthesis the compounds were tested for their antimicrobial activity by disk diffusion assay and MIC by broth micro dilution method against bacterial and fungal strains. Also, molecular docking studies have been performed on Peptide deformylase (PDF) of *E. coli* and CYP 450-14DM of *Candida albicans* to evaluate the possible mode of action of the molecules in the active site of the receptor.

2. Results and discussion

2.1. Chemistry

The long chain alkynoic acid and alkenoates used as the starting materials were prepared from the corresponding long chain alkenoic acids or fatty acids. The long chain alkynoic acid (**1**) was synthesized using the procedure of Kannan et al. [31]. The esters of fatty acids (**2**–**5**) (long chain alkenoates) were prepared by refluxing the fatty acid in methanol in the presence of catalytic amount of sulfuric acid (concentrated). Nitrobutane and 1,4-phenylene diisocyanate were purchased from Sigma Aldrich. Triethylamine, tetrahydrofuran (THF) and benzene were purchased from Merck, Mumbai. Nitrile oxide was generated in situ from nitrobutane employing 1,4-phenylene diisocyanate. The 1,3-dipolar cycloaddition of nitrile oxide to an alekene/alkyne gives an inseparable isomeric mixture of dihydroisoxazole/isoxazole derivatives. This transformation was most effective when excess base (3 equivalents of triethylamine) was employed and nitrobutane added dropwise over 6–8 h while heating. After refluxing, the reaction was quenched with water. The polyurea (polymer) was removed by filtration. Products were purified by column chromatography and identified using different spectral techniques. The signals of products in the ^{1}H and ^{13}C NMR spectra were successfully assigned. The high resolution mass (electron ionization) spectral studies have further confirmed their structures. The reaction sequences are outlined in Schemes 1 and 2.

IR spectrum of compound (**6**), 5-(carboxyoctyl)-3-propylisoxazole, revealed characteristic bands at 3285 (OH stretching), 2918 (CH stretching), 1702 (acid C=O stretching), 1465 (C=N stretching).^{1}H NMR peaks at 12.61 (1H, s, COO*H*), 6.98 (1H, s, C*H* ring), 2.35 (2H, t, J = 7.52 Hz, CH_2COOH), two triplets merged together at δ 2.18 were observed for four CH_2 protons alpha to isoxazole ring, 1.63 (2H, m, CH_2CH_2COOH), 1.54 (2H, m, $CH_2CH_2CH_3$), 1.28 (10H, br.s, CH_2 chain), 0.90 (3H, t, J = 7.21 Hz, CH_3). In ^{13}C NMR peaks at δ 176.18, 167.86, 82.17, 80.80, 44.26, 35.81, 32.68, 29.83, 29.68, 29.39, 29.01, 27.46, 25.61, 22.93, 14.10 were observed. The mass spectra showed characteristic molecular ion peak in accord with the molecular formula.

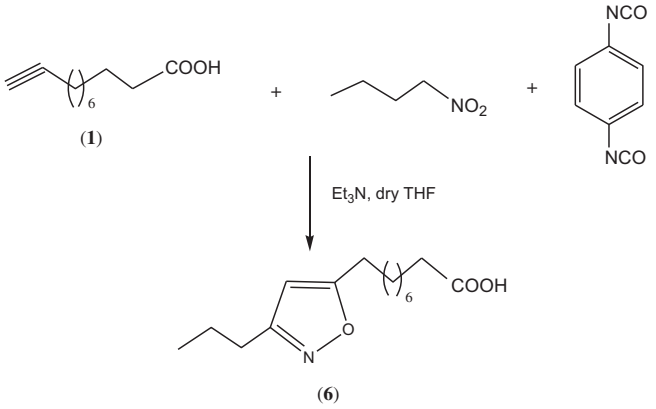

Scheme 1. Synthesis of 3,5-disubstituted isoxazole (**6**).

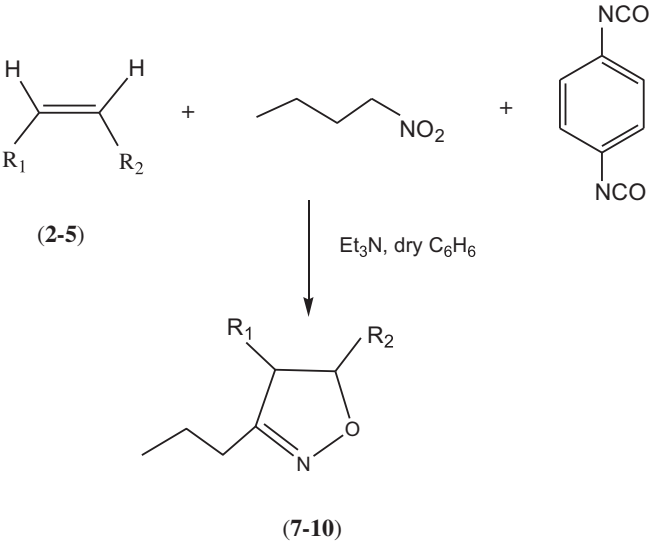

Compounds	R_1	R_2
2, **7**	H	$(CH_2)_8COOCH_3$
3, **8**	$CH_3(CH_2)_7$	$(CH_2)_7COOCH_3$
4, **9**	$CH_3(CH_2)_5CHOHCH_2$	$(CH_2)_7COOCH_3$
5, **10**	$CH_3(CH_2)_4$	$(CH_2)_2CHOH(CH_2)_7COOCH_3$

Scheme 2. Synthesis of 3,5-disubstituted and 3,4,5-trisubstituted-4,5-dihyroisoxazoles (**7**–**10**).

The structure of (**7**–**10**) is evident from their spectral data. The structure of compound (**7**) is outlined in Scheme 3. Compound (**7**), 5-(carbomethoxyoctyl)-3-propyl-4,5-dihyroisoxazole, showed IR absorption bands at 2931 cm^{-1} (CH stretching), 1740 cm^{-1} (ester C=O stretching), 1457 (C=N stretching). The ^{1}H NMR was more informative in assigning the structure. Diagnostic peaks for cyclic protons were appeared at 4.46 (1H, m, CH_2–*CH* ring), 2.91 (1H, dd,

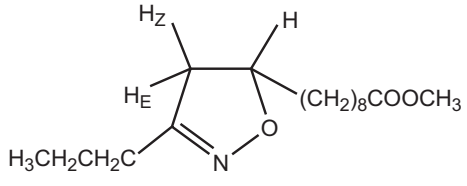

Scheme 3. Structure of 5-(carbomethoxyoctyl)-3-propyl-4,5-dihydroisoxazole (**7**).

J_{H_Z-H} = 16.70 Hz, $J_{H_Z-H_E}$ = 10.00 Hz, CH-CH_Z ring), 2.49 (1H, dd, J_{H_E-H} = 16.80 Hz, $J_{H_E-H_Z}$ = 8.10 Hz, CH–CH_E ring), 2.25 (4H, two triplets partially merged, $-CH_2COOCH_3$, $-CH_2CH_2CH_3$), 1.60 (6H, m, $CH_2CH_2CH_3$, $(CH_2)_5-CH_2-$, $CH_2CH_2COOCH_3$), 1.25 (10H, br.s, CH_2 Chain), 0.92 (3H, t, J = 7.30 Hz, CH_3). In ^{13}C NMR peaks at 174.23, 158.75, 79.97, 51.39, 42.01, 35.22, 34.01, 29.72, 29.32, 29.25, 29.17, 29.09, 25.51, 24.86, 19.74, 13.72 were observed. The mass spectra showed characteristic molecular ion peak in accord with the molecular formula. Similarly other compounds were characterized from their spectral data.

2.2. In silico study

2.2.1. Prediction activity spectra for substances (PASS)

A type of biological effects, toxicity, molecular mechanism and drug-likeness of compounds is presented in (Table 1). The high drug-likeness of the compounds (**9** and **10**) was determined to be 0.961 and 0.949 respectively which proved the high probability of these compounds as drugs. The antihypertensive activity of the compounds (**9** and **10**) predicted the pharmacological effect of these compounds. Moreover, it was shown that the algorithm used in PASS can successfully be applied to discriminate the drug-like compounds from drug-unlike substances.

2.2.2. ADME and toxicity prediction

The ADME-Plot is a 2D plot using calculated ADMET_PSA_2D and ADMET_A logp98 properties. The graph was plotted against ADMET_PSA_2D vs. ADMET_A logp98. Blood Brain Barrier (BBB) and Human Intestinal Absorption (HIA) plot (Fig. 1) was drawn using all the compounds. In BBB plot two compounds (**7** and **9**) were falling outside the 99% ellipse (undefined). Compounds (**6** and **7**) are central nervous system inactive compounds and blood brain barrier cannot be penetrated by these compounds. So, the chances of central nervous system toxicity are low or absent. As the compounds (**6**, **8** and **10**) fall inside the 99% ellipse, these would be CNS active and would be able to penetrate the BBB. In HIA (human intestinal absorption) plot all the compounds except (**7**) have fallen inside the 99% ellipse. Hence, these compounds are expected to possess good human intestinal absorption. The aqueous solubility plays a critical role in the bioavailability of the candidate drugs, and with the exception of compound (**7**) having low aqueous solubility level (level 1) as referred in (Table 2), all other derivatives are having good or optimal aqueous solubility levels. Except compounds (**6** and **10**), no other compounds showed liver toxicity. Our results indicate that all the compounds except (**6** and **10**) are non toxic to the liver (level 0, Table 2), and thus they experience significant first-pass effect. Similarly, all synthesized compounds are satisfactory with respect to CYP2D6 liver (with reference to Table 2), suggesting that all the compounds are non-inhibitors of CYP2D6 (Table 3). This indicates that all the synthesized compounds are well metabolized in Phase-I metabolism. The compounds (**6** and **10**) have ADMET plasma protein binding $\geq$90% and compounds (**7**, **8**, **9**) have $\geq$95%, clearly suggesting that most of the compounds have good bioavailability and are not likely to be highly bound to carrier proteins in the blood (refer to Tables 2 and 3). Finally, an interesting observation was that the non-hydroxy analog of 3,4,5-trisubstituted-4,5-dihydroisoxazole, that is, 5-(carbomethoxyheptyl)-4-octyl-3-propyl-4,5-dihydroisoxazole (compound **8**), was found to pass the entire ADMET test. All the parameters calculated are tabulated in (Table 3). These observations denote that all the synthesized compounds can reach the desired targets.

Toxicity screening of the ligands was performed by using the toxicity prediction extensible protocol and the results were tabulated in (Table 4). From these toxicity studies it was found that none of the ligands have shown mutagenicity and ligands like (**8** and **9**)

Table 1
PASS predicted but not reported activities (hidden potential) of all the synthesized compounds.

Comp.	Activity		Drug likeness	Pa	Pi
6	Pharmacological effect	Uric acid excretion stimulant	0.800	0.306	0.059
		Antihypertensive		0.217	0.104
	Molecular mechanism	Endothelin receptor antagonist		0.134	0.009
		Endothelin B receptor antagonist		0.141	0.018
		Endothelin A receptor antagonist		0.094	0.008
		Nitric oxide agonist		0.293	0.173
		Nitric oxide donor		0.052	0.041
		Angiotensin antagonist		0.022	0.020
		Angiotensin II receptor antagonist		0.020	0.020
		Endothelin converting enzyme inhibitor		0.134	0.086
7	Pharmacological effect	Antihypertensive	0.648	0.246	0.084
		Uric acid excretion stimulant		0.206	0.165
	Molecular mechanism	Endothelin receptor antagonist		0.122	0.013
		Endothelin B receptor antagonist		0.123	0.024
		Endothelin A receptor antagonist		0.083	0.010
		Nitric oxide agonist		0.276	0.212
		Nitric oxide donor		0.055	0.036
		Angiotensin antagonist		0.020	0.022
		Angiotensin II receptor antagonist		0.020	0.020
8	Pharmacological effect	Antihypertensive	0.884	0.396	0.028
		Uric acid excretion stimulant		0.198	0.179
		Angiotensin AT2 receptor antagonist		0.052	0.048
	Molecular mechanism	Alpha 2 adrenoreceptor antagonist		0.288	0.054
		Endothelin B receptor antagonist		0.136	0.019
		Endothelin receptor antagonist		0.111	0.017
		Endothelin A receptor antagonist		0.070	0.015
		Nitric oxide donor		0.075	0.020
		Nitric oxide agonist		0.262	0.246
		Angiotensin antagonist		0.028	0.013
		Angiotensin II receptor antagonist		0.025	0.013
		Endothelin converting enzyme inhibitor		0.121	0.119
9	Pharmacological effect	Antihypertensive	0.961	0.302	0.055
	Molecular mechanism	Alpha 2 adrenoreceptor antagonist		0.261	0.068
		Endothelin B receptor antagonist		0.138	0.019
		Endothelin receptor antagonist		0.091	0.028
		Nitric oxide donor		0.072	0.022
		Endothelin A receptor antagonist		0.061	0.020
10	Pharmacological effect	Antihypertensive	0.949	0.325	0.048
	Molecular mechanism	Alpha 2 adrenoreceptor antagonist		0.243	0.079
		Endothelin B receptor antagonist		0.129	0.021
		Nitric oxide donor		0.076	0.019
		Endothelin receptor antagonist		0.086	0.030
		Endothelin A receptor antagonist		0.057	0.024

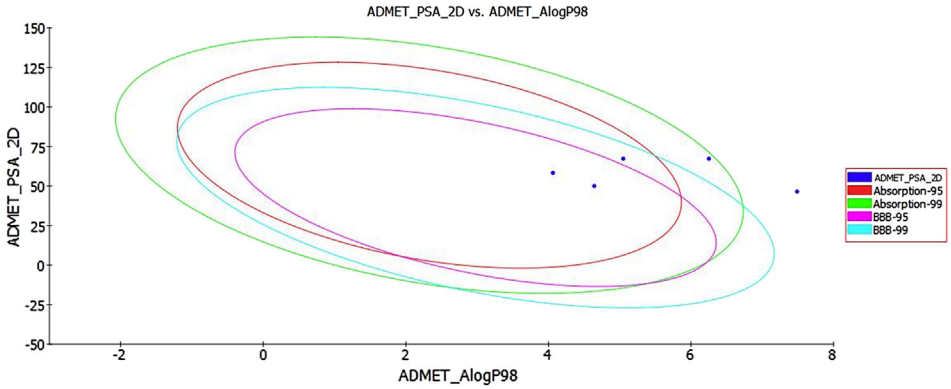

Fig. 1. Prediction of drug absorption for the synthesized compounds considered for anti-microbial activity. Discovery studio 2.5 ADMET Descriptors, 2D polar surface area (PSA 2D) in $Å^2$ for each compound is plotted against their corresponding calculated atom-type partition coefficient (ALogP98).

Table 2
Standard levels of ADMET descriptors from discovery studio 2.5.

Aq. Solubility and drug likeness		BBB		Cytochrome P450-14DM		Hepatotoxicity		Intestinal absorption	
Level	Intensity	Level	Intensity	Level	Value	Level	Value	Level	Value
0	Extremely low	0	Very high	0	Non inhibitor	0	Non toxic	0	Good
1	No, very low	1	High	1	Inhibitor	1	Toxic	1	Moderate
2	Yes, low	2	Medium	PPB				2	Poor
3	Yes, good	3	Low	Level	% of biding			3	Very poor
4	Yes, optimal	4	Very low	0	<90%				
5	No, too soluble	5	Warning: molecules with one or more unknown AlogP calculation	1	>90%				
6	Unknown			2	>95%				

have shown carcinogenic characters in female mouse models. No ocular irritancy, carcinogenicity and skin sensitization was found in national toxicity program (NTP) and food and drug administration (FDA) (Table 4).

2.2.3. Physicochemical properties prediction

In order to achieve good oral drugs we have subjected a series of long chain isoxazole derivatives (**6**–**10**) for the prediction of ADMET and Lipinski's "Rule of five" [32]. The ADMET parameters are a key parameter to understand the nature of interaction, between the concerned compound and its various targets.

2.2.3.1. pKa and log P. The octanol–water partition coefficient (*P*) (also referred to as Kow) is a measure of the propensity of a neutral compound to differentiate dissolution in these immiscible phases. Poor solubility and poor permeability are amongst the main causes for failure during drug development [33]. It is therefore, important to determine the physicochemical properties associated with a drug. Furthermore, there are hydrophobic binding sites on the proteins concerned in drug disposition further adding to the importance of lipophilicity. The results obtained are given in (Table 5). There also exists a good relationship between log P and antimicrobial activity and in this study we have found that compounds having higher log *P* and lower MIC values are the excellent antimicrobial agents. On the other hand, the molecules having higher MIC values and lower log *P* values are the least active as shown in (Fig. 2). The compounds with log *P* values close to the linear line and have lower MIC values are the most active.

Table 3
Computer aided ADME screening of the novel compounds.

Ligands	BBB level	Human intestinal absorption level	Aq. Solubility level	Hepatotoxicity level	CPY2D6 level	PPB level
6	1	0	3	3	0	1
7	4	3	1	0	0	2
8	1	0	3	0	0	2
9	4	1	2	0	0	2
10	1	0	2	1	0	1

BBB: Blood Brain Barrier, PPB: Plasma Protein Binding, CYP2D6: Cytochrome P450-14DM enzyme inhibition using 2D chemical structure as input.

2.2.3.2. "Rule of five" properties. For good oral bioavailability an ideal compound should have high oral bioavailability, good intestinal absorption and reduced molecular flexibility [34]. All the compounds of series (**6**–**10**) under investigation possessing less number of hydrogen bond donors (<5) and do possess a considerable number of acceptors (<10) as shown in (Table 5).

As shown in (Table 5), all parameters of the compounds were consistent with the 'rule of 5'. It was reported that a molecule with ten or fewer rotatable bonds and PSA less than 140 $Å^2$ might have a high probability of good oral bioavailability [35] as can be seen in (Table 5), all the compounds fulfilled both of the criteria.

2.2.3.3. The molar refractivity (MR). The molar refractivity (MR), which represents the size and polarizability of a molecule describing steric effects, was calculated (using ChemDraw Ultra 11.0 software) to explain the activity behavior of the synthesized novel molecules. It is obvious from (Table 5), that the higher value of molar refractivity favors the activity ratio of compounds (**9** and **10**).

2.2.4. Bioactivity score

The standard drug scores were compared with calculated scores of the synthesized compounds. Suitable modifications were made in order to achieve an active moiety, proper bioactivity and drug-likeness score as defined by Lipinski's rule. The bioactivity score for the synthesized derivatives are tabulated in (Table 6). In the

Table 4
Toxicity profile of the synthesized compounds using Toxicity Prediction – Extensible protocol of Accelrys discovery studio 2.5

Drugs	Mouse female NTP prediction	Mouse male NTP prediction	Rat female NTP prediction	Rat male NTP [prediction	Mouse female FDA prediction	Mouse male FDA prediction	Rat female FDA prediction	Rat male FDA prediction	WOE prediction	Ames prediction	DTP prediction	Skin irritancy	Skin sensitization	Ocular irritancy	Aerobic biodegradability prediction
6	Non-carcinogen	Non-carcinogen	Non-carcinogen	Non-carcinogen	Non-carcinogen	Single-carcinogen	Single-carcinogen	Non-carcinogen	Non-carcinogen	Non-mutagen	Toxic	Mild	None	None	Degradable
7	Non-carcinogen	Carcinogen	Non-carcinogen	Non-carcinogen	Non-carcinogen	Multi-carcinogen	Single-carcinogen	Non-carcinogen	Non-carcinogen	Non-mutagen	Toxic	Severe	None	None	Degradable
8	Carcinogen	Non-carcinogen	Non-carcinogen	Non-carcinogen	Non-carcinogen	Single-carcinogen	Non-carcinogen	Non-carcinogen	Non-carcinogen	Non-mutagen	Toxic	Severe	None	None	Degradable
9	Carcinogen	Non-carcinogen	Non-carcinogen	Non-carcinogen	Non-carcinogen	Multi-carcinogen	Non-carcinogen	Non-carcinogen	Non-carcinogen	Non-mutagen	Toxic	Severe	None	None	Degradable
10	Non-carcinogen	Carcinogen	Non-carcinogen	Non-carcinogen	Non-carcinogen	Non-carcinogen	Single-carcinogen	Single-carcinogen	Non-carcinogen	Non-mutagen	Non-toxic	Severe	None	None	Degradable

series, compounds (**9** and **10**) showed better GPCR ligand scores (0.19 and 0.19 respectively) than the standard drugs ciprofloxacin and fluconazole (0.12 and 0.12 respectively). Therefore, compounds (**9** and **10**) can be considered as the lead antimicrobial agents among the series.

2.3. In vitro antimicrobial activity

2.3.1. Antibacterial studies

The newly prepared compounds were screened for their antibacterial activity against *Escherichia coli* (ATCC-25922), *S. aureus*, *Pseudomonas aeruginosa* (ATCC-27853), *Streptococcus pyogenes* and *Klebsiella pneumoniae* (Clinical isolates) bacterial strains by disc diffusion method [36,37]. The susceptibility was assessed on the basis of the diameter of zone of inhibition against gram-positive and gram-negative strains of bacteria. Inhibition zones were measured and compared with the controls (Table 7).

Minimum inhibitory concentrations (MICs) were determined by broth micro dilution method. The nutrient broth, which contained logarithmic serially two fold diluted amount of test compound and controls were inoculated with approximately 5×10^5 c.f.u./ml of actively dividing bacteria cells. The cultures of the bacterial strains were incubated for 24 h at 37 °C and the growth was monitored visually and spectrophotometrically. The lowest concentration (highest dilution) required to arrest the growth of bacteria was regarded as minimum inhibitory concentration (MIC). To obtain the minimum bacterial concentration (MBC), 0.1 ml volume was taken from each tube and spread on agar plates. The number of c.f.u. was counted after 18–24 h of incubation at 35 °C. MBC was defined as the lowest drug concentration at which 99.9% of the inoculums were killed. The minimum inhibitory concentration and minimum bactericidal concentration are given in (Table 8).

The investigation of antibacterial screening data revealed that all the tested compounds showed moderate to good antibacterial activity. Among all the synthesized compounds, compound (**9**) showed highest antibacterial activity (25 μg/ml) nearly equivalent to standard drug ciprofloxacin. Compounds (**9** and **10**) showed good inhibition against *S. pyogenes*, *S. aureus* and *E. coli* species. In general, all the compounds were more effective against gram-positive bacteria as compared to gram-negative bacteria.

2.3.2. Antifungal assay

The stock solution of compounds was prepared in DMSO at a concentration of 200 mg/ml. Agar dilution assay and micro dilution method were used to establish the minimum inhibitory concentration (MIC) as well as minimum fungicidal concentration (MFC) of synthetic derivatives [38,39]. The results are presented in (Tables 9 and 10). As shown in (Table 9), compounds (**6**–**10**) had good antifungal effects against tested clinical species of *Candida*. Among all the synthesized compounds, compounds (**9** and **10**) showed excellent antifungal activity (32 μg/ml) against *Candida tropicalis* and *C. albicans*, which were resistant to fluconazole and itraconazole as well as against standard species of *Candida*.

2.4. Molecular modeling

The model for Cytochrome P450-14DM of *C. albicans* generated by modeller package using template structure human Cytochrome P450-14DM (PDB Id: 3LD6) with 39% sequence identity and 54% sequence similarity (Fig. 3). The model has only one residue in disallowed regions similar to that of the template as observed in the Ramachandran plot using Procheck program (http://nihserver.mbi.ucla.edu/SAVES/) (Table 11).

Ramachandran plot analysis showing the percentage of residues lying in each of the four different regions of Cytochrome P450-

Table 5
Physiochemical properties and rule of five parameters of synthesizes compounds.

Comp.	Chemical formula	Lipinski rule of 5				TPSA[d](A°2)	MSA[e]	Rotatable bonds	No. violations	Gibbs energy [kj/mol]	MR [cm^3/mol]	MV[f]
		miLog *P*[a]	MW	HBD[b]	HBA[c]							
6	$C_{15}H_{25}NO_3$	4.758	267.319	0	4	52.337	477.58	12	0	−150.68	80.05	290.7
7	$C_{16}H_{29}NO_3$	4.583	283.354	1	4	58.897	521.10	11	0	−220.68	74.68	279.3
8	$C_{23}H_{43}NO_3$	8.371	381.590	0	4	47.903	743.62	18	1	−127.49	112.63	414.71
9	$C_{23}H_{43}NO_4$	7.065	397.600	1	5	68.131	743.00	18	1	−266.75	114.09	422.217
10	$C_{23}H_{43}NO_4$	6.830	397.590	1	5	68.131	742.89	18	1	−266.75	114.09	422.217

Comp.	Henry's law	Heat of form [kJ/mol]	Elemental analysis calculated	Boiling point [K]	Melting point [K]	Log *D* (pH 7.4)	*C* Log *P*	pK[a]
6	4.15	−616.62	C (67.38%), H (9.42%), N (5.24%), O (17.95%)	732.78	451.72	4.27	4.4	4.6
7	2.61	−695.62	C (68.29%), H (9.67%), N (4.98%), O (17.06%)	788.38	541.2	4.45	4.0	4.7
8	1.26	−848.09	C (72.39%), H (11.36%), N (3.67%), O (12.58%)	879.46	508.85	7.66	8.1	4.5
9	1.26	−1005.6	C (69.4%), H (10.9%), N (3.52%), O (16.10%)	971.2	554.67	6.28	6.4	4.6
10	1.26	−1005.6	C (69.48%), H (10.9%), N (3.52%), O (16.10%)	971.2	554.67	6.28	5.9	4.5

[a] miLog *P*: the log *P* value calculated using molinspiration server.
[b] HBD: hydrogen bond donor (expressed as the sum of OH and NH).
[c] HBA: hydrogen bond acceptor (expressed as the sum of O and N atoms).
[d] TPSA: topological polar surface area (defined as a sum of the surfaces of polar atoms in a molecule).
[e] MSA: molecular surface area.
[f] MV: molecular volume.

14DM (Fig. 4). In the disallowed region, the number of residues is also given in brackets with percentage and all the results are summarized in (Table 11).

Molecular docking studies have been performed on Peptide deformylase (PDF) of *E. coli* and CYP 450 of *C. albicans* to predict the probable mode of action, of the molecules in the active site of the receptor. The binding of the compounds have been compared with the Ciprofloxacin binding site (Fig. 5).

2.4.1. Molecular docking of the synthesized compounds with S12 protein of 30S ribosomal subunit of E. coli

The potent activity of synthesized compounds (**6**–**10**) as new antimicrobial agents, prompted us to study the docking of these derivatives inside the active site of S12 protein of ribosomal subunit of *E. coli*, the potential target for antibacterial agents. X-ray study of 30S Ribosomal subunit S12 protein (PDB Id: 1FJG, L Chain) with

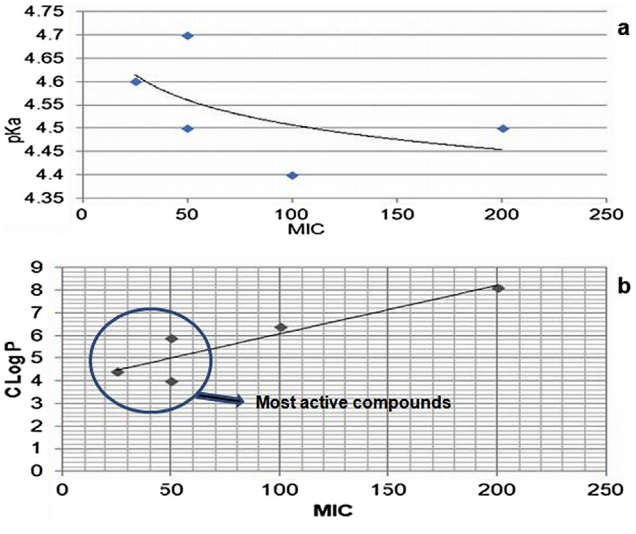

Fig. 2. (a) Graph showing correlation between the MIC for *E. coli* growth inhibition by 3-propylisoxazole and 3-propyl-4,5-dihydroisoxazoles and the computed pka values of the parent bases. The line is to guide the eye; (b) Graph showing correlation between log P and MIC values. The compounds whose log *P* values are close to the linear line and have lower MIC values are the most active. The most active compounds are encircled.

divergent inhibitors shows that the binding pocket of the enzyme includes the following residues, Arg89, Lys 46, Lys 47, and Lys91 as shown in the (Figs. 5 and 6). The top score pose was selected for each compound and their results were shown in (Table 12**)** and compared with ciprofloxacin, which was redocked with the target protein using the same protocol. It was evident from (Figs. 5 and 6) that for each compound, the binding site was found to be the same. It was interesting to observe that even though the core structure of all the compounds was same, the degree of interaction and binding location were found to be different for all the synthesized compounds. The binding sites of the compounds were found to be in close proximity to the binding site of ciprofloxacin as evident from (Figs. 5 and 6). The variation in the bioactivity is mainly attributed to the difference in their binding pattern. For instance, the bioactivity studies showed that compounds (**6** and **7**) showed comparable results with ciprofloxacin against gram-positive and gram-negative strains of bacteria. It may be due to two oxygen atoms from the carboxyoctyl side chain of compound (**6**) which had two hydrogen bonds with a terminal nitrogen atom of Arg89 (bond length 3.26 Å and 2.80 Å) one hydrogen bond with Lys46 (bond length 2.77 Å). Compound (**7**) also had three hydrogen bonds (Lys91 bond length 3.06 Å, Arg89; 3.06 Å and Lys46; 3.09 Å). In the similar fashion standard ciprofloxacin also interacted with the S12 protein and made two hydrogen bonds with Lys46 (bond length 2.68 Å and 2.98 Å) and Lys91 (bond length 2.67 Å. The compounds (**8**, **9**, and **10**) showed better bioactivity as compared to standard ciprofloxacin. Compound (**8**) had four hydrogen bonds (two hydrogen bonds with Arg89 having bond lengths 3.24 Å and 2.75 Å, one hydrogen bond with Lys46 having bond length of 3.29 Å and another hydrogen bond with Lys91 having a distance of 3.02 Å).

Table 6
Bioactivity score of the synthesized compounds.

Comp.	GPCR ligand	Ion channel	Modulator kinase	Protease inhibitor	Nuclear receptor ligand	Enzyme inhibitor
6	0.03	0.13	−0.43	0.06	−0.12	0.16
7	0.41	0.06	−0.78	−0.05	−0.06	0.25
8	0.13	0.05	−0.40	0.01	0.08	0.07
9	0.19	0.13	−0.33	0.14	0.20	0.20
10	0.19	0.11	−0.34	0.13	0.16	0.18
Cip.	0.12	−0.04	−0.07	−0.19	−0.21	0.28
Flu.	0.12	−0.04	−0.07	−0.19	−0.21	0.28

Cip. = Ciprofloxacin; Flu. = Fluconazole.

Table 7
Antibacterial activity of 3-propylisoxazole and 3-propyl-4,5-dihydroisoxazole derivatives.

Compounds	Diameter of zone of inhibition (mm)				
	Gram positive bacteria		Gram negative bacteria		
	S. pyogenes	*S. aureus*	*P. aeruginosa*	*K. pneumoniae*	*E. coli*
6	21.6 ± 0.4	19.2 ± 0.4	31.2 ± 0.4	18.3 ± 0.4	25.7 ± 0.4
7	20.2 ± 0.3	18.1 ± 0.4	30.1 ± 0.4	17.1 ± 0.3	25.1 ± 0.3
8	22.3 ± 0.4	21.6 ± 0.4	31.3 ± 0.4	18.5 ± 0.4	26.7 ± 0.4
9	23.2 ± 0.2	22.6 ± 0.4	32.5 ± 0.6	19.2 ± 0.3	27.6 ± 0.6
10	22.4 ± 0.4	20.8 ± 0.3	31.8 ± 0.4	18.9 ± 0.4	26.5 ± 0.3
Standard	23.0 ± 0.2	22.0 ± 0.2	32.0 ± 0.3	19.0 ± 0.2	27.0 ± 0.2
DMSO	–	–	–	–	–

Positive control (standard): ciprofloxacin; negative control: DMSO; antibacterial activity measured by the Halo Zone Test (Unit, mm).

In case of ribosomal subunit of S12 protein, the ligand (**9**) had maximum negative Glide score and contributed five hydrogen bonds (Fig. 6) followed by that of compounds (**10** and **8**) (Table 12). These compounds also showed better bioactivity results as compared to standard ciprofloxacin (Tables 7 and 8).

The S12 protein is necessary for the translational accuracy. This docking study proposes that these synthesized compounds have a similar affinity towards the ribosomal subunit of S12 protein of *E. coli* as that of the standard ciprofloxacin. Hence, all of these derivatives can easily dock in the active site residue of the S12 protein and form a docked complex and as a result prevent the translational accuracy of *E. coli*. This leads to the inhibition of formation of protein necessary for the transcription of *E. coli* and disturbs the self-defense mechanism of the *E. coli* species.

2.4.2. Molecular docking of the synthesized compounds with active site of Cytochrome P450-14DM of C. albicans

The binding site of ketoconazole (ligand present in the template) is used as the active site in the Cytochrome P450-14DM model (Fig. 7). The results show that the overall trend of the interaction energies of all the derivatives is in good qualitative agreement with the *in vitro* antifungal activities.

Ligand (**6**) had no hydrogen bond but possesses 50 hydrophobic interactions and show maximum Glide score of −9.92. Whereas, ligand (**7**) had one hydrogen bond in the active site residue at His 132 and carbomethoxy oxygen of carbomethoxyheptyl side chain (bond length 3.02 Å), and glide score of −6.01. As shown in (Fig. 8), compound (**8**) had no hydrogen bond but 72 hydrophobic interactions and higher binding score (7.59) as compared to that of control fluconazole (−7.44 kcal/mol).

Among all the synthesized compounds, ligand (**9**) had maximum negative Glide score as well as maximum binding energy with the active site of Cytochrome P450-14DM of *C. albicans* and contributed to maximum three hydrogen bonds (Fig. 8), followed by that of compound (**10**) which had two hydrogen bonds (Table 13). These compounds also showed better bioactivity results as compared to standard fluconazole (Tables 9, 10 and 13). Like standard drug fluconazole, in case of compound (**9**) one of the carbomethoxy oxygen was forming hydrogen bonding interaction with the residues of Cytochrome P450-14DM at Ser 378 (bond length 3.22 Å) and another with His 377 (bond length 3.24 Å). The third hydrogen bond was formed between the oxygen atom from the hydroxyl group on 2′-hydroxyoctyl side chain and Tyr 64 (bond length 3.08 Å).

In case of compound (**10**), oxygen atom from the dihydroisoxazole heterocylic ring forms H-bonding interactions with the residues Ser 378 (2.86 Å) and another hydrogen bond was formed between the oxygen atom of the hydroxyl group on 8′-hydroxycarbomethoxydecyl side chain and Ser 378 (bond length 2.86 Å) of Cytochrome 450-14DM. It suggests that the affinity of all the synthesized compounds to the potential receptor Cytochrome P450-14DM may primarily attributed to their hydrogen and non-bonding interaction with the apoprotein part of the active site. The binding mode of the long chain isoxazole derivatives with the active site of Cytochrome P450-14DM provides a reasonable explanation for their antifungal activities. The antifungal activities of all the compounds are comparable to the control fluconazole. These results suggest that the addition of the alkyl/carboxyalkyl/carbomethoxyalkyl/hydroxyalkyl/hydroxycarbomethoxy alkyl side chains with 5–10 carbon atoms are optimal for antifungal activities and binding of these inhibitors to the Cytochrome P450-14DM receptor. The S4 subsite is a hydrogen bond donor and acceptor region, which interacts with the functional groups (carboxyl group, carbomethoxy group and hydroxyl group) on the 3-propylisoxazole and 3-propyl dihydroisoxazole ring. To study the effect of substituents at 3-propylisoxazole and 3-propyl dihydroisoxazole heterocyclic ring on their antifungal activities, the analogs with different side chains i.e. alkyl/carboxyalkyl/carbomethoxyalkyl/hydroxyalkyl/hydroxycarbomethoxyalkyl were designed and synthesized. The binding mode of the docked molecules to Cytochrome P450-14DM and their corresponding antifungal activities suggest that compounds with hydrogen bonding donor or acceptor substituent like hydroxyl group exhibit higher antifungal activities than compounds (**6** and **8**).

2.5. Structure activity relationship (SAR)

The physicochemical properties MW, MV, MR and log P of the compounds (**6**–**10**) are presented in (Table 5). The compounds (**7**, **9** and **10**) form hydrogen bonds with the target proteins of *C. albicans*. Correspondingly, all the compounds have hydrogen bond interaction with the S12 protein of *E. coli*. The structural activity study shows that antimicrobial activity is dependent on the oxygen atom

Table 8
MIC and MBC results of 3-propylisoxazole and 3-propyl-4,5-dihydroisoxazole derivatives.

Compounds	Gram positive bacteria				Gram negative bacteria					
	S. pyogenes		*S. aureus*		*P. aeruginosa*		*K. pneumoniae*		*E. coli*	
	MIC	MBC	MIC	MBC	MIC	MBC	MIC	MBC	MIC	MBC
6	50	100	50	100	100	>100	50	>100	50	100
7	50	100	50	>100	100	>100	100	>100	100	>100
8	25	50	25	100	25	50	25	100	25	50
9	25	50	25	50	25	50	25	100	25	50
10	25	50	25	100	50	100	25	100	25	100
Standard	12.5	12.5	6.25	12.5	12.5	25	6.25	25	6.25	12.5

MIC (μg/ml) = minimum inhibitory concentration, i.e. the lowest concentration of the compound to inhibit the growth of bacteria completely; MBC (μg/ml) = minimum bacterial concentration, i.e., the lowest concentration of the compound for killing the bacteria completely. Positive control: ciprofloxacin.

Table 9
In vitro antifungal activity of all the synthesized compounds (**6**–**10**) against standard species of *Candida*.

Comp.	Tested fungi (MIC 90% and MFC μg/ml)											
	C. albicans		*C. tropicalis*		*C. glabrata*		*C. parapsilosis*		*C. kruzei*		*C. dubliniensis*	
	MIC	MFC	MIC	MFC	MIC	MFC	MIC	MFC	MIC	MFC	MIC	MFC
6	>256	>256	>256	>256	128	>256	128	>256	>256	>256	128	256
7	>256	>256	>256	>256	>256	>256	>256	>256	>256	>256	>256	>256
8	128	256	128	>256	128	>256	>256	>256	>256	>256	128	>256
9	128	256	64	>256	32	256	32	128	64	128	32	256
10	128	>256	128	>256	64	128	32	>256	128	>256	128	>256
Flu.	>256	>256	32	256	8	128	4	32	32	>256	2	>256
It.	>256	>256	>256	>256	0.12	>256	0.6	0.5	0.6	0.12	>256	>256

Flu. = Fluconazole, It. = Itraconazole.

Table 10
In vitro antifungal activity of all the synthesized compounds (**6**–**10**) against clinical species of *Candida*.

Comp.	Tested fungi (MIC 90% and MFC μg/ml)									
	C. albicans		*C. tropicalis*		*C. parapsilosis*		*C. albicans**		*C. tropicalis**	
	MIC	MFC	MIC	MFC	MIC	MFC	MIC	MFC	MIC	MFC
6	>256	>256	128	>256	256	>256	>256	>256	>256	>256
7	>256	128	>256	128	>256	>256	>256	>256	>256	>256
8	128	>256	128	>256	128	>256	>256	>256	>256	128
9	32	256	64	256	128	>256	128	>256	>256	>256
10	64	256	64	>128	128	>256	>256	>256	>256	>256
Flu.	8	>256	16	256	0.5	1	R	R	R	R
It.	0.12	>256	1	>256	0.25	0.5	R	R	R	R

Flu. = Fluconazole, It. = Itraconazole, * = resistant to fluconazole and itraconazole, R = resistant.

of isoxazole heterocyclic ring as well as on the nature of the substituent (hydroxyl group, carboxyl group and carbomethoxy group) on heterocyclic ring's side chains. Moreover, these compounds, in most of the cases, exhibited favorable calculated SAR parameters: rather high octanol–water partition coefficient (log *P*) and low values (below 140 Å^2) of polar surface area (PSA) that is linked closely to higher bioavailability. This fact strongly prompted us to study these derivatives as potential new antimicrobial substances. The most favorable values of log P and PSA were found for all the compounds due to the presence of isoxazole heterocyclic ring in their structures.

Among compounds (**6** and **7**), compound (**6**) showed better antibacterial activity compared to compound (**7**) due to the presence of isoxazole ring and carboxyoctyl side chain. In case of compound (**8**), the dihydroisoxazole ring contains propyl, octyl and carbomethoxyheptyl side chain. Whereas, in compound (**9**), dihydroisoxazole ring is substituted with propyl, hydroxyoctyl and carbomethoxyheptyl side chains and in compound (**10**), dihydroisoxazole ring is substituted with propyl, pentyl and hydroxycarbomethoxydecyl side chains. The dihydroisoxazole derivatives containing hydroxyl group substituted side chains (compounds **9** and **10**) showed better activity compared to isoxazole/dihydroisoxazole derivatives containing non-hydroxy side chain (compounds **6**, **7** and **8**) as they make more hydrogen bonds due to presence of hydroxyl group substituted side chains. The presenters of hydroxyl groups on alkyl/carbomethoxyalkyl side chains were crucial in making the stable complexes through hydrogen bond and hydrophobic interactions within the active site of the selected

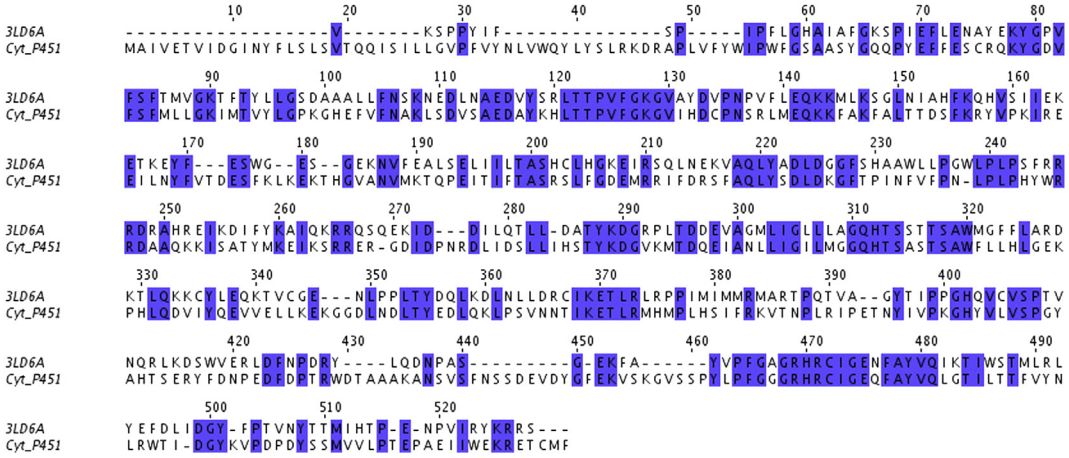

Fig. 3. Alignment of Cytochrome P451 of *C. albicans* with the template (PDB id: 3LD6). The conserved residues are highlighted in blue color. (For interpretation of the references to color in this figure legend, the reader is referred to the web version of this article.)

Table 11
Procheck analysis for quality of model of Cat1.4 with the template.

	Ramachandran plot analysis			
	Most favorable	Additional allowed	Generously allowed	Disallowed
Cyt P450-14DM	87.4%	10.4%	1.9%	0.2% (1)
Template	92.1%	7.6%	0.0%	0.3% (1)

targets in the bacteria and fungi. The compounds (**9** and **10**) showed better docked complex, physiochemical parameter and higher binding energy compared to standard drugs ciprofloxacin and fluconazole.

Among all the compounds, compounds (**8**, **9** and **10**) have high drug-likeness score and high values of high octanol–water partition coefficient (log P) indicating these derivatives as better antimicrobial agent compared to compounds (**6** and **7**). The Clog *P* values were influenced enough by the presence of the hydroxyl group on alkyl/carbomethoxyalkyl side chains. A good *in vitro* activity of all the compounds was described to their strong binding energies coupled with a high lipophilic character, which allows an optimal penetration into the cytosol. Even though the compounds (**9** and **10**) are endowed with good interaction energies, an increasing hydrophilic character positively affects their ability to cross the membrane of the bacteria and fungi. The lipophilic character of all the synthesized compounds combined with very low PSA values may be the main factor ensuring a good level of distribution *in vivo*. PSA values were in the range between 47.903 and 68.131 $Å^2$ (Table 5).

3. Conclusions

The proposed method for the synthesis of novel long chain isoxazole derivatives was simple and all the synthesized compounds obtained in good yield. Prediction of the biological activity of these compounds by using the PASS software was successful to some extent. The report of the study confirms traditional usage of these compounds as antimicrobial agents. However, large data must be generated through the pharmacognostic studies before going for commercialization. The physicochemical parameters suggested that most of the compounds possessed drug-like properties. In general, the results showed there was a dependency between biological activity and lipophilicity, where MIC decreased with increasing lipophilicity. This present study showed that all the title compounds were exhibiting antibacterial activities. These compounds were evaluated against yeast. Among the synthesized compounds, compounds (**9** and **10**) showed antimicrobial activity against all tested microorganisms which is almost equivalent to the standard drugs ciprofloxacin and fluconazole. Also, compounds (**9** and **10**) had antifungal activity against tested clinical species of *Candida* which were resistant to fluconazole as well as itraconazole. The results of the docking experiments for the newly synthesized compounds (**6**–**10**), with the 30s ribosomal subunit were found to be in accordance with the *in vitro* antimicrobial activity data obtained. The binding sites of the compounds were found to be in close proximity to the binding site of the standard drug ciprofloxacin. It was interesting to observe that even though the core structure of all the compounds was the same, the degree of interaction and binding patterns were found to be different. We anticipate that this kind of docking and antipathogenic screening studies would help in designing of novel drugs that targets microbial protein synthesis. Moreover, the mode of action of the long chain isoxazole and dihydroisoxazole derivatives showed that the affinity of the lead molecules for Cytochrome P450-14DM was mainly attributed to hydrogen and their non-bonding interaction with the active site residues of Cytochrome P450-14DM protein and binding with the heme, which was similar to that of azoles antifungal agents. The studies presented here provide a new structural type for the development of novel antifungal agents.

4. Experimental protocol

4.1. Physical and spectroscopic measurements

Anhydrous conditions were achieved by drying flasks and other equipments in the oven. Reagents and solvents were of commercial grade and were used without further purification. Undec-10-enoic and (Z)-octadec-9-enoic acids were obtained commercially from Fluka Chemical (Switzerland). (9Z, 12R)-12-Hydroxyoctadec-9-enoic (Ricinolic) and (9R, 12Z)-9-hydroxyoctadec-12-enoic (Isoricinolic) acids were isolated from the natural sources, i.e. from *Ricinus communis* and *Wrighteria tinctoria* seed oils, respectively following Gunstone's partition method [40] and further purified by column chromatography. Thin layer chromatography (TLC) was

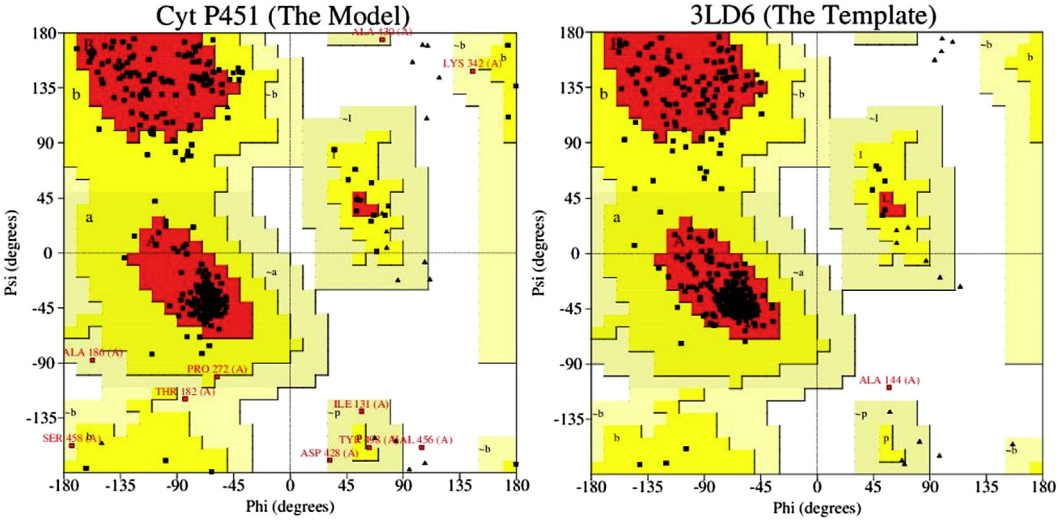

Fig. 4. Ramachandran Plots for the model and the template. Ramachandran Plots are obtained as output by using PROCHECK software.

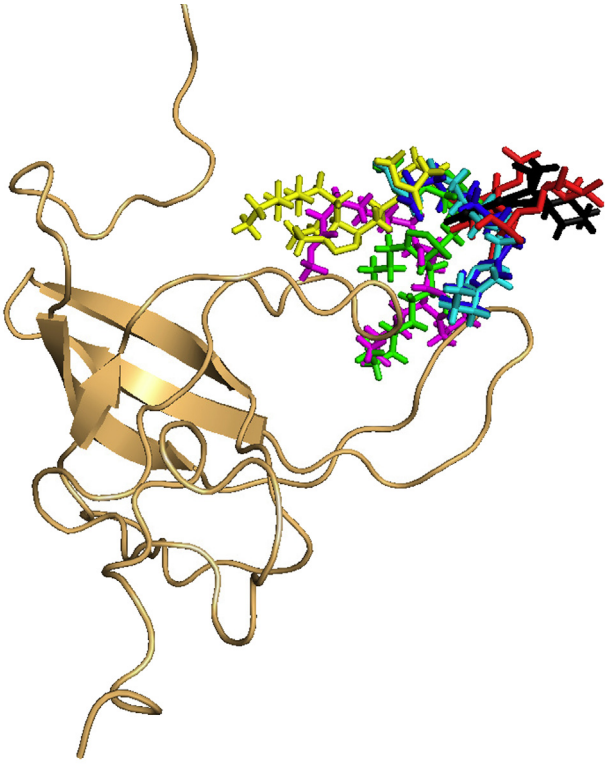

Fig. 5. All the five molecules docked in the binding site of S12 protein. The protein is in cartoon representation and the ligand molecules are in sticks colored as compound (**6**), blue; compound (**7**), cyan; compound (**8**), yellow; compound (**9**), green; compound (**10**), magenta and control drug Ciprofloxacin, black. The original bound ligand Streptomycin is also shown in sticks colored red. (For interpretation of the references to color in this figure legend, the reader is referred to the web version of this article.)

performed on glass plates (20-5 cm) with a layer of silica gel (Merck, Mumbai, India 0.5 mm thickness) and was visualized in an iodine chamber. Silica gel (60–80 mesh) was used for column chromatography. The eluent was a mixture of diethyl ether/ethyl acetate and petroleum ether in different proportions for different compounds. Solvents were dried and distilled before use. IR spectra were obtained by Shimadzu 8201 PC FT-IR uses KBr pellet with absorption given in cm^{-1}. ^1H NMR spectra were recorded in $CDCl_3$ on a Bruker DRX-400 instrument. The chemical shifts (δ) were measured relative to TMS as an internal standard and are quoted in ppm. Coupling constants (J) are expressed in Hertz (Hz). ^{13}C NMR spectra were recorded at the Bruker DRX-400 spectrometer in $CDCl_3$ with $CDCl_3$ ($\delta = 77.00$).

4.2. Synthesis of compounds

4.2.1. General procedure for the synthesis of long chain alkynoic acid (**1**)

The long chain alkynoic acid (**1**) which is used as the starting material was prepared by the previously reported method [31].

*4.2.1.1. Synthesis of 3,5-disubstituted isoxazole derivative of long chain alkynoic acid (**6**).* 1,4-Phenylene diisocyanate (0.003 mol) was added to long chain alkynoic acid (**1**) (0.001 mol) in dry tetrahydrofuran (THF) (20 ml). Triethylamine (0.003 mol) was added to the reaction mixture and this was heated to 80 °C. Nitrobutane (0.003 mol) was added in portions over a period of 6–8 h, and then the reaction was heated for additional 2 h. The precipitate was observed. After heating, the reaction mixture was cooled. The reaction was quenched with water (≈6 ml) and then allowed to stir at room temperature for 1 h. The polyurea (polymer) was removed by filtration and washed with THF. The solvent was evaporated on a water bath and then worked up with diethyl ether-water. Further, product (**6**) was purified by silica gel column with petroleum ether/diethyl ether as eluent. The characterization data of novel compound (**6**) are given below.

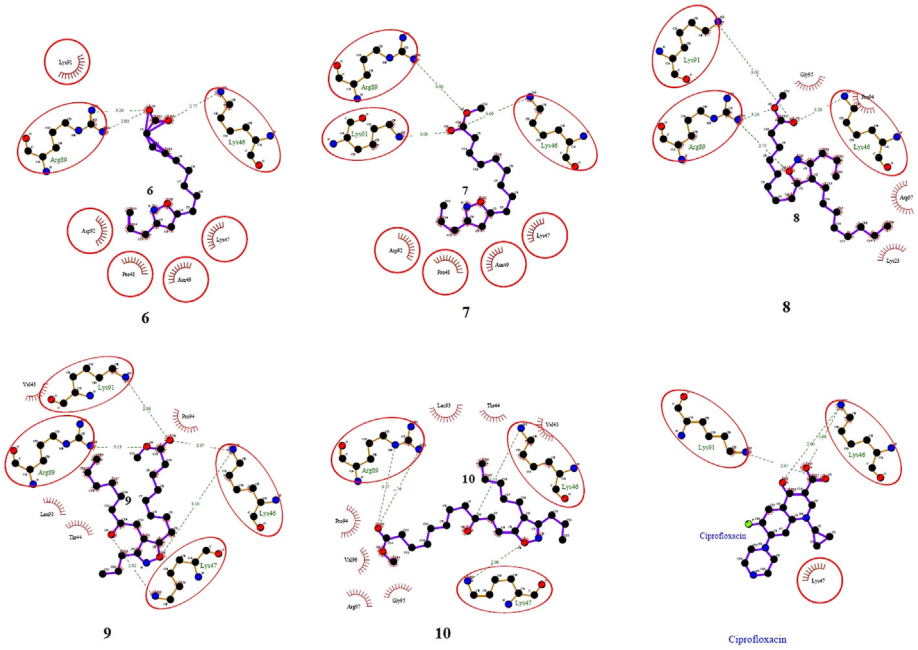

Fig. 6. The interaction plot (Ligplot) of all the five molecules with the binding site residues of S12 protein. The panel 1–5 corresponds to compounds (**6**–**10**) respectively and panel 6 to control drug Ciprofloxacin. The hydrogen bonds and hydrophobic interactions are shown which are holding the ligand within the binding site.

Table 12
The ligand molecules with number of molecular interactions and the scores for strength of binding.

S12 protein					
Comp.	Hydrogen bonds	Hydrophobic interactions	Glide score	Binding energy (kcal/Mol)	Log (K_d)
6	3 (2)	29 (7)	−1.97	−5.39	3.95
7	3 (3)	19 (7)	0.87	−5.40	3.96
8	4 (3)	34 (6)	−2.14	−6.18	4.53
9	5 (4)	31 (8)	−1.25	−5.75	4.22
10	4 (3)	28 (10)	−0.64	−6.19	4.54
Cipro.	3 (2)	10 (3)	−1.50	−5.69	4.17

The number of residues involved in the hydrogen & hydrophobic interactions are provided in brackets with the total number of interactions the molecule is experiencing. The binding energy and -log (K_d) values are calculated using X-Score. The more negative is the glide score, the better is the docking. Cipro.: Ciprofloxacin.

*4.2.1.2. 5-(Carboxyoctyl)-3-propylisoxazole (**6**).* White solid; M.P = 79–80 °C; yield: 80%; IR (KBr, cm^{-1}): 3285 (OH stretching), 2918 (CH stretching), 1702 (C=O stretching), 1465 (C=N stretching). ^{1}H NMR ($CDCl_3$, δ_H): 12.61 (1H, s, COO*H*), 6.98 (1H, s, C*H* ring), 2.35 (2H, t, *J*=7.52 Hz, CH_2COOH), 2.18 (4H, two triplets merged together, $(CH_2)_5$–CH_2, $CH_3CH_2CH_2$), 1.63 (2H, m, CH_2CH_2COOH), 1.54 (2H, m, $CH_2CH_2CH_3$), 1.28 (10H, br.s, CH_2 chain), 0.90 (3H, t, J = 7.21 Hz, CH_3). ^{13}C NMR ($CDCl_3$, δ_C): 176.18, 167.86, 82.17, 80.80, 44.26, 35.81, 32.68, 29.83, 29.68, 29.39, 29.01, 27.46, 25.61, 22.93, 14.10. MS (ESI): m/z = 290.210 $[M + Na]^+$, calculated = 290.308.

*4.2.2. Synthesis of 3,5-disubstituted and 3,4,5-trisubstituted-4,5-dihydroisoxazole derivatives of long chain alkenoates (**7**–**10**)*

1,4-Phenylene diisocyanate (0.03 mol), nitrobutane (0.01 mol) and long chain alkenoates (**2**–**5**) (0.01 mol) were dissolved in dry benzene (30 ml). Triethylamine (25-50 drops) was added. The reaction mixture became turbid and a precipitate was observed. After 8 h at reflux the reaction mixture was cooled. The reaction was quenched with water (≈5 ml) and allowed to stir at room temperature for 1 h. The polyurea (polymer) was removed by filtration and washed with benzene. The solvent was evaporated on a water bath and then worked up with diethyl ether-water. Further, the products (**7**–**10**) were purified by silica gel column with petroleum ether/diethyl ether as eluent. All these novel compounds were characterized from their spectral data.

*4.2.2.1. 5-(Carbomethoxyoctyl)-3-propyl-4,5-dihydroisoxazole (**7**).* Colorless oily liquid; yield: 85%; IR (KBr, cm^{-1}): 2931 (CH stretching), 1740 (C=O stretching), 1457 (C=N stretching). ^{1}H NMR ($CDCl_3$, δ_H): 4.46 (1H, m, CH_2–C*H* ring), 3.60 (3H, s, OCH_3), 2.91 (1H, dd, J_{H_Z-H} = 16.70 Hz, $J_{H_Z-H_E}$ = 10.00 Hz, CH–CH_Z ring), 2.49 (1H, dd, J_{H_E-H} = 16.80 Hz, $J_{H_E-H_Z}$ = 8.10 Hz, CH–CH_E ring), 2.25 (4H, two triplets partially merging, CH_2COOCH$_3$, $CH_2CH_2CH_3$), 1.60 (6H, m, $CH_2CH_2CH_3$, $(CH_2)_5$–CH_2, CH_2CH_2COOCH$_3$), 1.25 (10H, br.s, CH_2 Chain), 0.92 (3H, t, J = 7.30, CH_3). ^{13}C NMR ($CDCl_3$, δ_C): 174.23, 158.75, 79.97, 51.39, 42.01, 35.22, 34.01, 29.72, 29.32, 29.25, 29.17, 29.09, 25.51, 24.86, 19.74, 13.72. MS (ESI): m/z = 305.700 $[M + Na]^+$, calculated = 306.343.

*4.2.2.2. 5-(Carbomethoxyheptyl)-4-octyl-3-propyl-4,5-dihydroisoxazole (**8**).* Colorless oily liquid; yield: 83%; IR (KBr, cm^{-1}): 2928 (CH stretching), 1743 (C=O stretching), 1462 (C=N stretching). ^{1}H NMR ($CDCl_3$, δ_H): 5.26 (2H, m, *H*C-C*H* ring), 3.59 (3H, s, O–CH_3), 2.54 (2H, t, J = 7.60 Hz, CH_2COOCH$_3$), 2.42 (2H, t, J = 7.60 Hz, $CH_2CH_2CH_3$), 1.95 (4H, m, H_2C–CH–CH–CH_2), 1.70 (2H, m, CH_2CH_2COOCH$_3$), 1.56 (2H, m, $CH_2CH_2CH_3$), 1.20 (20H, br.s, CH_2 Chain), 0.91 (3H, t, J = 7.20 Hz, $CH_2CH_2CH_3$), 0.81 (3H, dist.t, CH_3). ^{13}C NMR ($CDCl_3$, δ_C): 173.82, 159.24, 80.18, 52.85, 43.01, 35.55, 34.89, 31.28, 30.97, 29.98, 29.86, 29.69, 29.40, 29.27, 29.10, 26.67, 25.38, 24.46, 22.73, 18.89, 13.96. MS (ESI): m/z = 404.190 $[M + Na]^+$, calculated = 404.504.

*4.2.2.3. 5-(Carbomethoxyheptyl)-4-[(2′R)-2′-hydroxyoctyl]-3-propyl-4,5-dihydroisoxazole (**9**).* Yellow oily liquid; yield: 80%; IR (KBr, cm^{-1}): 3328 (OH stretching), 2924 (CH stretching), 1738 (C=O stretching), 1447 (C=N stretching). ^{1}H NMR ($CDCl_3$, δ_H): 5.32 (2H, m, *H*C–C*H* ring), 4.20 (1H, m, C*H*–OH), 3.60 (3H, s, O–CH_3), 2.65 (2H, t, J = 7.54 Hz, CH_2COOCH$_3$), 2.35 (2H, t, J = 7.45 Hz, $CH_2CH_2CH_3$), 2.10 (4H, m, H_2CHC–CHCH_2), 1.80 (1H, m, CH–O*H*), 1.68 (2H, m, CH_2CH_2COOCH$_3$), 1.42 (2H, m, $CH_2CH_2CH_3$), 1.30 (18H, br.s, CH_2 chain), 0.95 (3H, t, J = 7.25 Hz, $CH_2CH_2CH_3$), 0.87 (3H, dist.t, CH_3). ^{13}C NMR ($CDCl_3$, δ_C): 176.41, 158.70, 80.01, 72.19, 52.85, 43.41, 39.56, 35.60, 34.84, 29.99, 29.75, 29.51, 29.39, 29.28, 29.01, 27.48, 25.40, 24.91, 21.99, 19.57, 14.00. MS (ESI): m/z = 420.409 $[M + Na]^+$, calculated = 420.503.

*4.2.2.4. 5-[(8′R)-8′-Hydroxy(carbomethoxydecyl)]-4-pentyl-3-propyl-4,5-dihydroisoxazole (**10**).* Yellow oily liquid; yield: 75%; IR (KBr, cm^{-1}): 3294 (OH stretching), 2918 (CH stretching), 1734 (C=O stretching), 1468 (C=N stretching). ^{1}H NMR ($CDCl_3$, δ_H): 5.34 (2H, m, *H*C–C*H* ring), 4.41 (1H, m, C*H*–OH), 3.69 (3H, s, O–CH_3), 2.55 (2H, t, J = 7.45 Hz, CH_2COOCH$_3$), 2.29 (2H, t, J = 7.50 Hz, $CH_2CH_2CH_3$), 1.98 (4H, m, H_2CHC–CHCH_2), 1.78 (1H, m, CH–O*H*), 1.67 (2H, m, CH_2CH_2COOCH$_3$), 1.40 (2H, m, $CH_2CH_2CH_3$), 1.30 (18H, br.s, CH_2 chain), 0.96 (3H, t, J = 7.25 Hz, $CH_2CH_2CH_3$), 0.87 (3H, dist.t, CH_3). ^{13}C NMR ($CDCl_3$, δ_C): 175.43, 156.96, 81.00, 73.16, 51.87, 42.05, 39.02, 34.90, 34.29, 29.82, 29.69, 29.47, 29.37, 29.29, 29.00, 26.83,

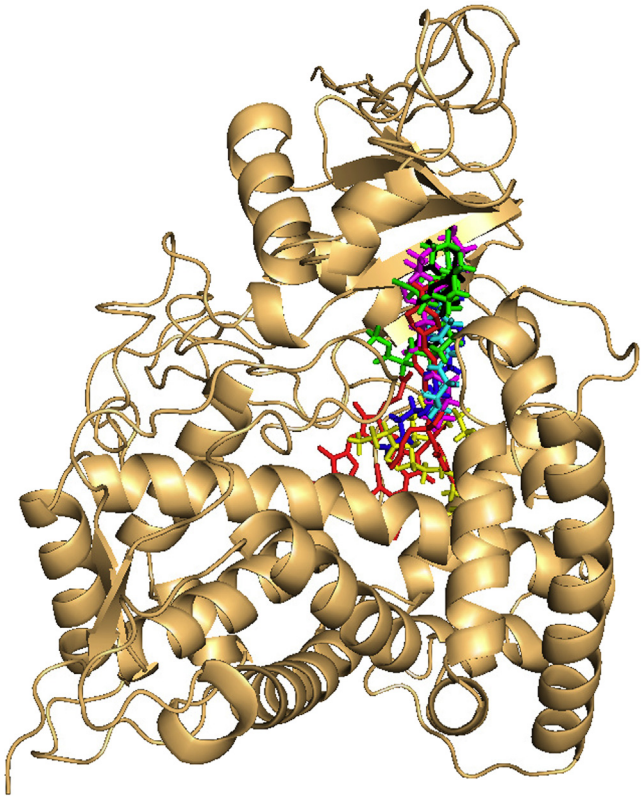

Fig. 7. All the five molecules docked in the binding site of Cytochrome P451 of *C. albicans*. The protein is in cartoon representation and the ligand molecules are in sticks colored as compound (**6**), blue; compound (**7**), cyan; compound (**8**), yellow; compound (**9**), green; compound (**10**), magenta and a control drug Fluconazole in black. Heme and bound ligand, Ketoconazole, are also shown in sticks colored red. (For interpretation of the references to color in this figure legend, the reader is referred to the web version of this article.)

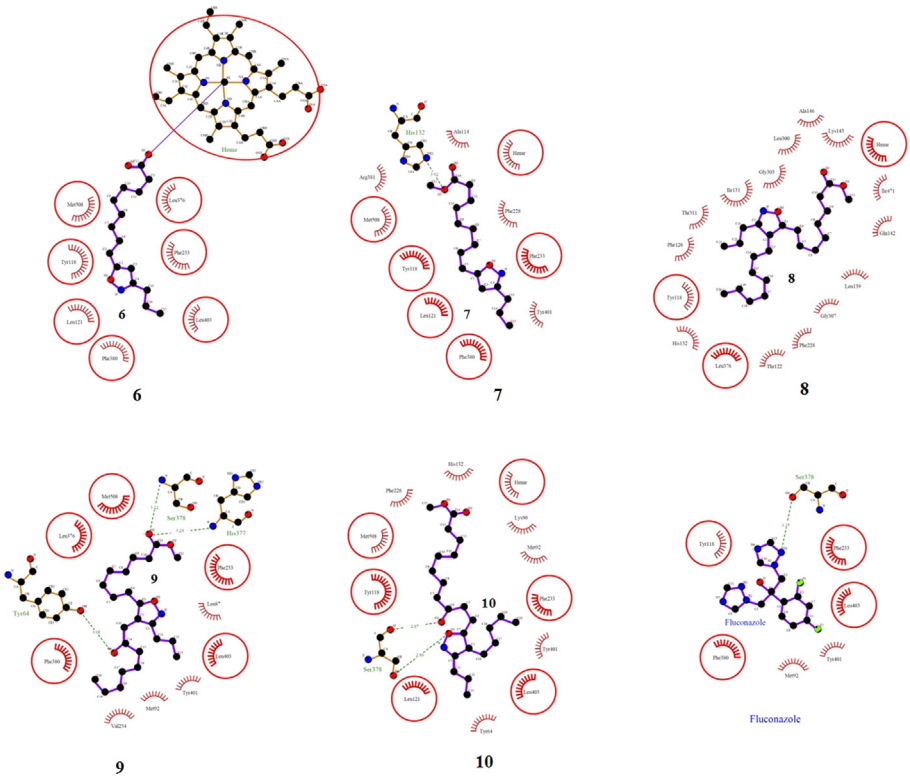

Fig. 8. The interaction plot (Ligplot) of all the five molecules with the binding site residues of Cytochrome P450-14DM of *C. albicans*. The panel 1–5 corresponds to compounds (**6**–**10**) respectively whereas panel 6 shows control drug Fluconazole. The hydrogen bonds and hydrophobic interactions are shown which are holding the ligand within the binding site.

24.98, 23.99, 21.90, 19.81, 13.93. MS (ESI): $m/z = 420.347$ $[M + Na]^+$, calculated = 420.503.

4.3. Prediction of hidden biological potential of the synthesized compounds

The activity of the molecule was predicted, using PASS (Prediction of Activity Spectra for Substances) which estimates the probable biological activity profiles for compounds under study based on their structural formulas presented in .MOLfile or .SDfile format using Marvin applet [41].

4.4. ADME & toxicity studies

In silico ADME studies were performed by using ADME Descriptors algorithm of Accelrys Discovery studio 2.5 in which various pharmacokinetic parameters like Aq. Solubility [42], human intestinal absorption [43], plasma protein binding (PPB) [44]; blood brain barrier (BBB) penetration [45], Cytochrome P450-14DM inhibition [46] and hepatotoxicity levels [47] were estimated for 5 ligands. Obtained results were cross checked with the standard levels listed in (Table 2). Toxicity profiling of all the 5 ligands were performed by employing toxicity prediction-extensible protocol of Accelrys discovery studio 2.5.

Toxicity profile includes screening for aerobic biodegradability, developmental toxicity potentials, AMES mutagenicity, carcinogenicity, and ocular & skin irritancy [48]. Teratogenicity effects of the ligands were studied by using an online tool, OSIRIS property explorer [49].

Table 13
The ligand molecules with number of molecular interactions and the scores for strength of binding.

Cytochrome P450-14DM protein					
Molecule	Hydrogen bonds	Hydrophobic interactions	Glide score	Binding energy (kcal/Mol)	Log (K_d)
6	0	50 (8)	−9.92	−7.20	5.28
7	1	57 (11)	−6.01	−7.37	5.40
8	0	72 (17)	−5.95	−7.59	5.56
9	3 (3)	48 (12)	−8.76	−8.46	6.20
10	2 (2)	51 (13)	−8.38	−8.69	6.37
Flu.	1	22 (7)	−6.26	−7.44	5.46

The number of residues involved in the hydrogen & hydrophobic interactions are provided in brackets with the total number of interactions the molecule is experiencing. The binding energy and -log (K_d) values are calculated using X-Score. The more negative is the glide score, the better is the docking. Flu.: Fluconazole.

4.5. Prediction of physicochemical properties

The octanol–water partition coefficient Clog*P* being a measure of hydrophobicity/lipophilicity was calculated using ChemDraw Ultra 11.0 software (Cambridgesoft Corporation) [50]. The physicochemical parameters including octanol partition coefficients (miLog *P*), MW, HBD, HBA, TPSA, and Rotatable bonds were calculated using a Molinspiration server (http://www.molinspiration.com/cgi-bin/properties) and ChemAxon (chemicalize.org).

4.6. Bioactivity score

The drugs were also checked for the bioactivity by calculating the activity score. All the bioactivity parameters were checked with the help of software ChemSketch 11 and Molinspiration drug-likeness score online (www.molinspiration.com).

4.7. Antibacterial assay

The antibacterial activity of the synthesized compounds was completed by the disk diffusion method and measured by Halo

Zone Test [36,37]. The MIC of synthesized compounds against bacterial strains was performed by the micro dilution test and the results were observed visually and spectrophotometrically.

4.8. Antifungal assay

Bacterial and fungal strains were obtained from microbiology laboratory as gift, where these strains were already characterized. Sabouraud dextrose agar (SDA), potato dextrose agar (PDA), oatmeal, and RPMI 1640 were used for agar dilution and macrodilution methods. The clinical isolates of fungi including *C. albicans*, *C. tropicalis*, *and Candida parapeilosis* were purified and subcultures on SC, SCC, and PDA media before testing. To obtain the stock solutions of the compounds, 200 mg/ml of the compound was dissolved in DMSO. The compounds were diluted in solid and broth media to obtain a final concentration from 0.0312 to 256 mg/ml, using PDA and RPMI 1640 media. The inocula of the yeasts were prepared from 1 to 10 days mature colonies grown.

4.9. Molecular modeling and docking

4.9.1. Modeling of Cytochrome P450-14DM from C. albicans

Homology model of Cytochrome P450-14DM was generated using Modeller9v9 package [51]. Human Cytochrome P450-14DM protein was chosen as the template (PDB id: 3LD6) which displayed 39% identity and 54% similarity with the sequence of our protein. The five best models out of 100 models were shortlisted based on the lowest value of the Modeller objective function or the DOPE assessment score and with the highest GA341 assessment score. Finally, the best model was selected using Procheck analysis [52] and thus the best chosen model has shown the presence of only one residue in the disallowed region similar to that of the template as revealed by Ramachandran plot.

4.9.2. Protein & grid preparation

The crystal structure of 30S Ribosomal subunit S12 (PDB Id: 1FJG, L Chain) was retrieved from protein data bank and the modeling of Cytochrome P450-14DM was performed and the best model is selected. Proteins are prepared in Schrodinger protein preparation wizard including the addition of hydrogen atoms followed by minimization and optimization using the OPLS force field in the premin option of Schrodinger Glide [53]. The shape and properties of the receptor are represented on a grid by several different sets of fields that provide progressively more accurate scoring of the ligand poses. For S12 protein, the grid is generated for the site containing Streptomycin whereas for Cytochrome P450-14DM protein, the binding site of ketoconazole is used as a clue for grid generation.

4.9.3. Ligand preparation

All the ligands were then prepared in Schrodinger ligprep wizard and predocking preparations were made where hydrogens were added followed by minimization and optimization in OPLS_2005 force field, finally 10 conformations for each ligand were generated and set ready for docking.

4.9.4. Docking of all five ligands on S12 protein and Cytochrome P450-14DM

Docking was performed after preparation of ligand library, proteins and the grid in binding site of proteins. Our chosen software Glide uses Systematic and Simulation method for searching the poses and ligand flexibility. In systematic method it uses incremental construction for searching, and its output G score is a combination of various parameters. The G score is calculated as:

$$\text{G} - \text{Score} = \text{H bond} \pm \text{Lipo} \pm \text{Metal} \pm \text{Site} \pm 0.130\text{Coul} \pm 0.065\nu\text{d}W - \text{BuryP} - \text{RotB}.$$

where: H bond = Hydrogen bonds, Lipo = hydrophobic interactions, Metal = metal-binding term, Site = polar interactions in the binding site, VdW = Vander-waals forces, Coul = columbic forces, Bury P = penalty for buried polar group, Rot B = freezing rotable bonds. As each ligand has 10 stereoisomers or conformations, so each conformation was subjected to extra precision (XP) module for detailed docking.

4.9.5. Post docking analysis

For analyzing the interaction of docked protein-ligand complex, Ligplot program was used to check the polar and hydrophobic interaction between the receptor and ligand [54]. PyMOL was used in preparation of figures showing protein-ligand complex and also in the analysis of ligand–protein interactions [55]. X-Score is used for calculating the binding energy and $-\log(K_d)$ for each ligand [56].

Acknowledgments

The authors wish to thank the Chairman, Department of Chemistry, Aligarh Muslim University, Aligarh for providing necessary research facilities and SAIF, Panjab University, Chandigarh for Spectral services. Two of us (AA[1] and HV[1]) thank to CSIR and DST, New Delhi for awarding Junior Research Fellowship (JRF). In part, research is also supported by UGC-SAP(DRS-I) funds.

Appendix A. Supplementary data

Supplementary data related to this article can be found at http://dx.doi.org/10.1016/j.ejmech.2013.10.051.

References

[1] R.A. Devasia, T.F. Jones, J. Ward, L. Stafford, H. Hardin, C. Bopp, M. Beatty, E. Mintz, W. Schaffner, Am. J. Med. 119 (2006) 168–176.
[2] D.J. Diekema, B.J. BootsMiller, T.E. Vaughn, R.F. Woolson, J.W. Yankey, E.J. Ernst, S.D. Flach, M.M. Ward, C.L.J. Franciscus, M.A. Pfaller, B.N. Doebbeling, Clin. Infect. Dis. 38 (2004) 78–85.
[3] B.C. Herold, L.C. Immergluck, M.C. Maranan, D.S. Lauderdale, R.E. Gaskin, S. Boyle-Vavra, C.D. Leitch, R.S. Daum, JAMA 279 (1998) 593–598.
[4] W. Zhang, E.M. Berberoy, J. Freeling, D. He, R.A. Moxley, D.H. Francis, Infect. Immun. 74 (2006) 3107–3114.
[5] J.S. Yoder, S. Cesario, V. Plotkin, X. Ma, K. Kelly-Shannon, M.S. Dworkin, Clin. Infect. Dis. 42 (2006) 1513–1517.
[6] A.S. Puerto, J.G. Fernandez, J.D.L.D. Castillo, M.J.S. Pino, G.P. Angulo, Diagn. Microbiol. Infect. Dis. 54 (2006) 135–139.
[7] C.M. Nolan, E.G. Chalhub, D.G. Nash, T. Yamauchi, Antimicrob. Agents Chemother. 16 (1979) 171–175.
[8] A.E.A. Porter, A.R. Katritzky, C.W. Rees (Eds.), Comprehensive Heterocyclic Chemistry, vol. III, Pergamon, New York, 1984, pp. 157–197.
[9] A. Ahmad, A.U. Khan, Eur. J. Obstet. Gynecol. Reprod. Biol. 144 (2009) 68–71.
[10] H. Van de Waterbeemd (Ed.), Pharmacokinetic Challenges in Drug Discovery, Ernst-schering Research Foundation Workshop Series No. 37, Springer, 2001, pp. 213–234.
[11] P. Buchwald, N. Bodor, Drugs Future 27 (2002) 577–588.
[12] D.H. Sohn, Y.C. Kim, S.H. Oh, E.J. Park, X. Li, B.H. Lee, Phytomedicine 10 (2003) 165–169.
[13] Y. Pan, B. Cai, K. Wang, S. Wang, S. Zhou, X. Yu, B. Xu, L. Chen, J. Ethnopharmacol. 124 (2009) 98–102.
[14] D. Simoni, G. Grisolia, G. Giannini, M. Roberti, R. Rondanin, L. Piccagli, R. Baruchello, M. Rossi, R. Romagnoli, F.P. Invidiata, S. Grimaudo, M.K. Jung, E. Hamel, N. Gebbia, L. Crosta, V. Abbadessa, A. Di Cristina, L. Dusonchet, M. Meli, M. Tolomeo, J. Med. Chem. 48 (2005) 723–736.
[15] J.J. Talley, D.L. Brown, J.S. Carter, M.J. Graneto, C.M. Koboldt, J.L. Masferrer, W.E. Perkins, R.S. Rogers, A.F. Shaffer, Y.Y. Zhang, B.S. Zweifel, K. Seibert, J. Med. Chem. 43 (2000) 775–777.
[16] K. Karthikeyan, V.T. Seelan, K.G. Lalitha, P.T. Perumal, Bioorg. Med. Chem. Lett. 19 (2009) 3370–3373.

[17] E.I. Klimova, M.G. Marcos, T.B. Klimova, A.T. Cecilio, A.T. Ruben, R.R. Lena, J. Organomet. Chem. 585 (1999) 106–114.
[18] E. Wagner, L. Becan, E. Nowakowska, Bioorg. Med. Chem. 12 (2004) 265–272.
[19] M.P. Bourbeau, J.T. Rider, Org. Lett. 8 (2006) 3679–3680.
[20] L. Cecchi, F. De Sarlo, F. Machetti, Eur. J. Org. Chem. (2006) 4852–4860.
[21] M.F.A. Adamo, D. Donati, E.F. Duffy, P. Sarti-Fantoni, J. Org. Chem. 70 (2005) 8395–8399.
[22] S. Dadiboyena, E.J. Valente, A.T. Hamme II, Tetrahedron Lett. 51 (2010) 1341–1343.
[23] R. Huisgen, Angew. Chem. 75 (1963) 604–637.
[24] A.P. Kozikowski, Acc. Chem. Res. 17 (1984) 410–416.
[25] T. Mukaiyama, T. Hoshino, J. Am. Chem. Soc. 82 (1960) 5339–5342.
[26] E.J. Kantorowski, S.P. Brown, M.J. Kurth, J. Org. Chem. 63 (1998) 5272–5274.
[27] A. Rauf, M.R. Banday, R.M. Mattoo, Acta Chim. Slov. 55 (2008) 448–452.
[28] M.W.Y. Khan, F. Ahmad, I. Ahmad, S.M. Osman, J. Am. Oil. Chem. Soc. 60 (1983) 949–950.
[29] V.P. Mujeebur-Rahman, S. Mukhtar, W.H. Ansari, G. Lemiere, Eur. J. Med. Chem. 40 (2005) 173–184.
[30] S.M. Ahmed, F. Ahmad, S.M. Osman, J. Am. Oil. Chem. Soc. 62 (1985) 1578–1580.
[31] H. Kannan, M.W. Roomi, M.R. Subbaram, K.T. Achaya, Fette Seifen Anstrichm. 69 (1967) 644–646.
[32] C.A. Lipinski, F. Lombardo, B.W. Dominy, P.J. Feeney, Adv. Drug Deliv. Rev. 23 (1997) 3–25.
[33] U. Norinder, C.A.S. Bergstrom, Chem. Med. Chem. 1 (2006) 920–937.
[34] H.H.F. Refsgaard, B.F. Jensen, P.B. Brockhoff, S.B. Padkjaer, M. Guldbrandt, M.S. Christensen, J. Med. Chem. 48 (2005) 805–811.
[35] D.F. Veber, S.R. Johnson, H.Y. Cheng, B.R. Smith, K.W. Ward, K.D. Kopple, J. Med. Chem. 45 (2002) 2615–2631.
[36] R. Cruickshank, J.P. Duguid, B.P. Marmion, R.H.A. Swain, in: , twelfth ed.Medicinal Microbiology, vol. II, Churchill Livingstone, London, 1975, pp. 196–202.
[37] A.H. Collins, Microbiological Methods, second ed., Butterworth, London, 1976.
[38] Y. Liu, G. Tortora, M.E. Ryan, H.M. Lee, L.M. Golub, Antimicrob. Agents Chemother. 46 (2002) 1455–1461.
[39] T. Yashida, K. Jono, K.J. Okonoji, Antimicrob. Agents Chemother. 41 (1997) 1349–1351.
[40] F.D. Gunstone, J. Chem. Soc. (1954) 1611–1616.
[41] M.R. Bhandarkar, A. Khan, J. Ethnopharmacol. 91 (2004) 61–64.
[42] A. Cheng, K.M. Merz Jr., J. Med. Chem. 46 (2003) 357235–357280.
[43] W.J. Egan, K.M. Merz Jr., J.J. Baldwin, J. Med. Chem. 43 (2000) 3867–3877.
[44] G. Colmenarejo, A. Alvarez-Pedraglio, J.L. Lavandera, J. Med. Chem. 44 (2001) 4370–4378.
[45] J. Kelder, P.D. Grootenhuis, D.M. Bayada, L.P. Delbressine, J.P. Ploemen, Pharm. Res. 16 (1999) 1514–1519.
[46] R.G. Susnow, S.L. Dixon, J. Chem. Inf. Comput. Sci. 43 (2003) 1308–1315.
[47] A. Cheng, S.L. Dixon, J. Comput. Aided. Mol. Des. 17 (2003) 811–823.
[48] X. Xia, E.G. Maliski, P. Gallant, D. Rogers, J. Med. Chem. 47 (2004) 4463–4470.
[49] M. Sravani, N. Duganath, D.R. Gade, C.H.S. Reddy, Asian J. Res. Chem. 5 (2012) 153–158.
[50] A. Lagunin, D.A. Filimonov, Y.V. Borodina, A.A. Lagunin, A. Kos, Cur. Phar. Des. 16 (2010) 1703–1717.
[51] A. Sali, T.L. Blundell, J. Mol. Biol. 234 (1993) 779–815.
[52] R.A. Laskowski, M.W. MacArthur, D.S. Moss, J.M. Thornton, J. Appl. Crystallogr. 26 (1993) 283–291.
[53] R.A. Friesner, J.L. Banks, R.B. Murphy, T.A. Halgren, J.J. Klicic, D.T. Mainz, M.P. Repasky, E.H. Knoll, M. Shelley, J.K. Perry, D.E. Shaw, P. Francis, P.S. Shenkin, J. Med. Chem. 47 (2004) 1739–1749.
[54] A.C. Wallace, R.A. Laskowski, J.M. Thornton, Protein Eng. 8 (1995) 127–134.
[55] W.L. DeLano, The PyMOL Molecular Graphics System, DeLano Scientific, San Carlos, CA, 2002.
[56] R. Wang, L. Lai, S. Wang, J. Comput. Aided. Mol. Des. 16 (2002) 11–26.